

Analysis and Seismic Isolation of an Older Reinforced Concrete Vaulted Building

Stefano Sorace

Polytechnic Department of Engineering and Architecture
Via delle Scienze 206 33100 Udine, Italy

Gloria Terenzi

Department of Civil and Environmental Engineering
Via di S. Marta 3, 50139 Florence, Italy

Copyright © 2016 Stefano Sorace and Gloria Terenzi. This article is distributed under the Creative Commons Attribution License, which permits unrestricted use, distribution, and reproduction in any medium, provided the original work is properly cited.

Abstract

Reinforced concrete (R/C) structures designed with earlier Technical Standards often require retrofit interventions to improve their performance capacities, especially against seismic actions. A case study belonging to this class, i.e. the swimming pool building of the Naval Academy in Leghorn, Italy, rebuilt in 1948 after being destroyed by air raids during the Second World War, is examined herein. The structure of the main hall is constituted by a prefabricated R/C vaulted roof designed by the world-famous Italian engineer Pier Luigi Nervi, supported by a set of inclined columns with relatively small sections. The assessment analysis in current conditions shows unsafe response conditions of these members, as well as of several other columns and beams, under seismic action scaled at the basic design earthquake level. In order to minimize the impact of the retrofit intervention on the exposed structural elements, a base isolation solution is proposed for the building. The verification analyses in protected conditions highlight a substantial enhancement of the seismic response capacities of the structure, with no intervention required in the elevation structure, up to the maximum considered normative earthquake level.

Keywords: Older R/C structures, Seismic assessment; Base isolation

1 Introduction

The study of heritage-listed reinforced concrete (R/C) buildings, and particularly

the ones built in the so-called “golden age” period between the 1930s and the 1960s, is currently a challenging topic both in the fields of structural engineering [1] and history and conservation of modern architecture [2].

From a structural viewpoint, these buildings highlight poor performance capacities in comparison to the requirements of the latest normative generation, especially regarding the response to seismic actions. This is generally checked in terms of strength and ductility, and often translational stiffness, for frame structures. In addition, a lack of redundancy is noticed in certain special structures, including platform and vaulted roofs, arcades, stands, galleries, exhibition halls, tanks, bell towers, etc, where the number of vertical members is kept to a minimum and their cross sections are optimized in size, so as to improve the effects of geometrical slenderness. This imposes to carry out careful structural assessment analyses, as well as to plan seismic retrofit interventions, particularly when these buildings are of public use [1,3–5].

A representative case study belonging to this class of special structures, designed by the world-famous engineer Pier Luigi Nervi, is examined in this paper. The building is the swimming pool of the Naval Academy in Leghorn, Italy, whose first storey was rebuilt in 1948, after being destroyed by air raids during the Second World War (Fig. 1).

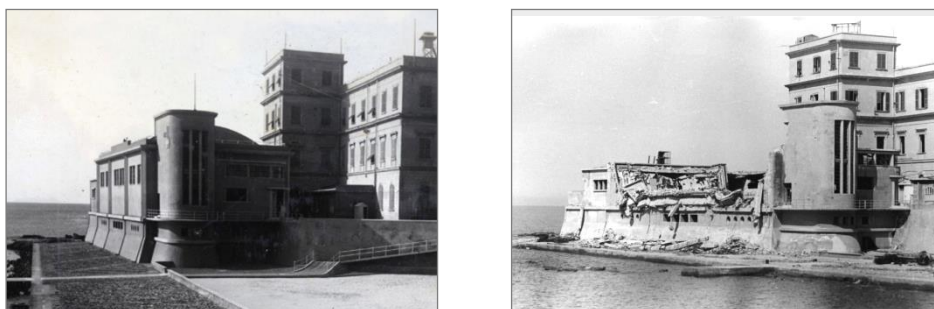


Fig. 1. Views of the original building (1936) and its appearance after the Second World War bombing (1945).

The distinguishing structural and architectural feature of the building is represented by the barrel vault-shaped roof, constituted by thin prefab R/C curved beams with smoothed-V wavy section, patented by Nervi during the construction works (patent No. 445781 registered on August 26th, 1948). This type of beams was adopted by the designer in the following decades for other roof vaults with greater spans, the first time in the Exhibition Hall Palace in Turin, in 1949, so that it has become a typical feature of the internationally recognized Nervi's style.

The other main structural members, i.e. the R/C columns and beams supporting the roof and the façade aisles — originally designed for gravitational loads only and pursuing a minimal size philosophy with respect to the calculated stress states — have small cross sections. This significantly contributes to the architectural elegance of the building, which was included in the Italian modern

heritage listing shortly after its construction. At the same time, these characteristics can remarkably affect the seismic performance of the structural system. Furthermore, the presence of a brick masonry stairwell wing situated in eccentric position in plan determines noticeable torsional contributions to the modal response of the building.

Based on these observations, a seismic assessment study was carried out in the frame of a research line developed by the authors on modern heritage R/C structures and infrastructures [1, 5]. The results highlight the unsafe response of several members at the basic design earthquake level, and near-critical conditions at the maximum considered earthquake level. An advanced retrofit hypothesis is proposed to obtain safe response conditions up to the latter level. The solution consists in incorporating a seismic isolation system on top of the columns bearing the pool tank, and at the bottom of the columns of the pool hall and the stairwell and entrance masonry wings. This allows minimizing the impact of the retrofit intervention on the exposed structural elements, as well as exploiting the unusual presence of a frame structure supporting the pool tank, originally built to protect it against floods from the sea and from an adjacent stream.

A synthesis of the construction history of the building and its structural characteristic, the results of the assessment analyses, and the base isolation retrofit design hypothesis are presented in the next sections.

2 Construction history of the building

The construction works of the swimming pool building of the Naval Academy started in 1934. The site is situated on Leghorn seaside, adjacent to the mouth of Rio Maggiore stream. A preliminary reclamation of the site was carried out to reach firmer soil conditions. A continuous R/C wall was built as retaining structure, on the bank side, and as perimeter wall of the basement of the building, on the seaside. The pool tank was built within this enveloping wall, supported by an underlying R/C frame structure (Fig. 2). This uplifted position with respect to the foundation soil was adopted to protect the pool tank against any possible floods from the sea and the stream, as well as against the rise of groundwater.

The swimming pool building was provided with a R/C frame structure standing on the box wall of the basement. The stairwell and entrance wings, situated in lateral position with respect to the pool hall, have a brick masonry structure. The stair flights are made of R/C slabs, supported by four R/C columns.

The bombings suffered by the Naval Academy in 1944 completely destroyed the swimming pool hall, whereas the stairwell and entrance wings were only slightly damaged (Fig. 1).

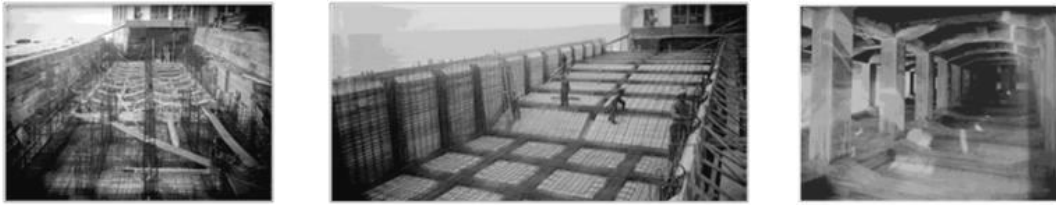


Fig. 2. Views of the construction works of the R/C basement and the pool tank, and the completed under-pool structure (1935).

In the aftermath of the Second World War, the Italian Ministry of Defence approved the reconstruction of the pool hall. The design was assigned to Pier Luigi Nervi, who conceived a barrel vault-shaped R/C structure for the roof, with span of 11.4 m, supported by a set of inclined columns. As mentioned in the Introduction, the vault is constituted by thin prefab R/C curved beams with smoothed-V wavy section (Fig. 3). The beams are 300 mm high and 50 mm thick, with radius of curvature equal to 6.8 m and length equal to 1/2 of the vault span. The reinforcement consists of a mesh of steel wires, integrated by a set of Ø5 longitudinal bars. A transversal R/C diaphragm and a ribbed contour are built at both ends, to connect the beams one to another and to the supporting columns during the installation works (Fig. 3). The connection is obtained by means of 4 Ø8 bars placed at the bottom of the V-shaped section, and 4 Ø8 bars on the two top ribs, embedded in on-site integrative casts (for which the roof beams constitute the formworks). A transversal diaphragm is located at the mid-span as stiffening element in this direction, whereas the beams are stiffened by the two continuous top ribs in longitudinal direction (Fig. 3).

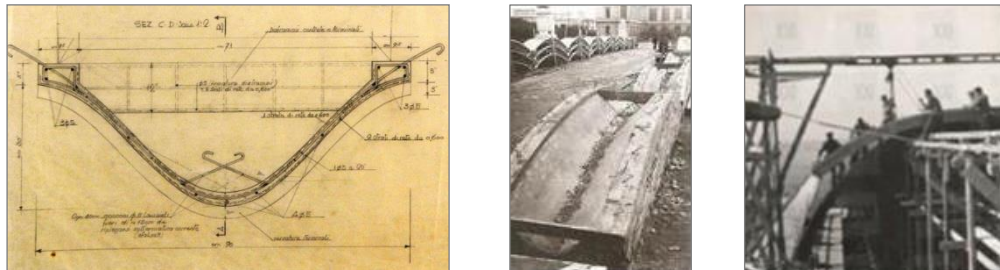


Fig. 3. Original design drawing of a prefab R/C curved element of the barrel vault roof, and views of the on-site manufacturing and installation works (1947-1948).

The structural plans of the under-pool, basement and ground floors, and the longitudinal and transversal cross sections of the building are shown in Figs. 4 and 5, respectively. Over time, the building has been the object of routine maintenance interventions only, mainly concerning waterproofing and technical plants. An external and an internal view in current conditions are displayed in Fig. 6.

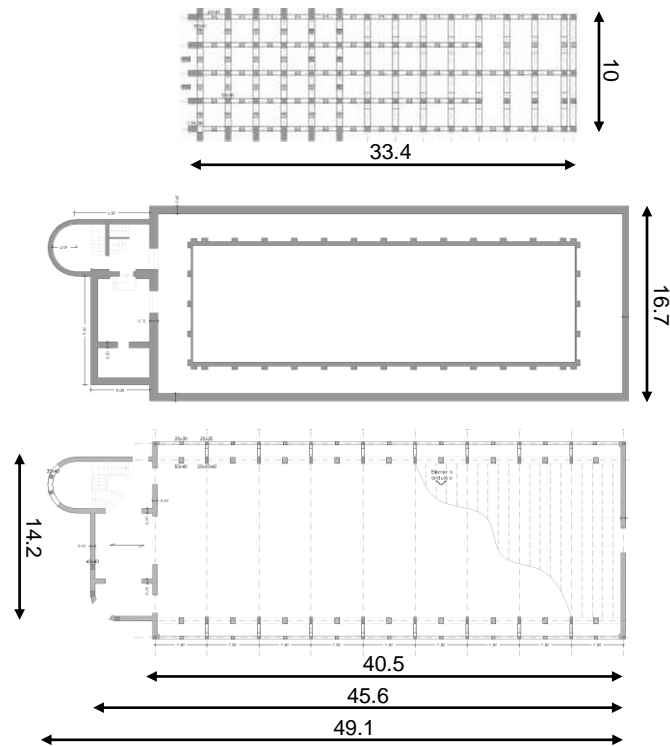


Fig. 4. Structural plans of the under-pool, basement and ground floors (dimensions in meters).

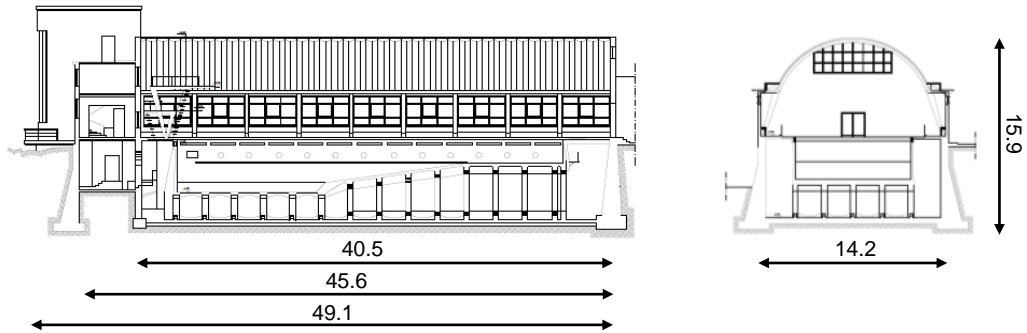


Fig. 5. Longitudinal and transversal cross sections (dimensions in meters).

The dimensions of the cross sections of the remaining structural elements are as follows: the roof columns have a base of 250 mm and height varying from 400 mm, at the bottom, to 600 mm, on top; the façade columns and stairwell columns have mutual section of (250×250) mm×mm; the roof-supporting beams and the façade beams have mutual section of (500×400) mm×mm and (250×300) mm×mm, respectively; the under-pool columns have section of (500×500) mm×mm, except for a set of perimeter elements situated below the deepest portion of the pool tank, with section of (500×1300) mm×mm; the under-pool beams have sections of (500×400) mm×mm or section of (400×400) mm×mm, enlarged in proximity to the

beam-to-column joints to absorb the maximum bending and shear stresses safely; the perimeter walls of the basement are 700 mm thick, with vertical stiffening ribs of different dimensions in the longitudinal and transversal sides; finally, all brick masonry walls are 300 mm thick.



Fig. 6. Current views of the building.

The mechanical properties of concrete and steel, and the reinforcement details have also been deduced from the original design drawings and characterization test reports. These documents highlight that the compressive cube strength of concrete, $f_{c,cube}$, is not lower than 35 MPa for the roof beams, and 25 MPa for the remaining structural members. Reinforcing steel is in smooth bars with a minimum yield stress, $f_{y,min}$, equal to 230 MPa. The compressive and tensile strengths of masonry, f_{cm} and f_{tm} , are fixed at 4 MPa and 0.15 MPa, respectively. Considering that no diagnostic activities were carried out on the structural elements in this study, the values of the mechanical parameters were divided by a confidence coefficient, FC , equal to 1.2 in stress state checks, according to the prescriptions of the Commentary on the Italian Technical Standards [6] with regard to existing structures, in addition to the basic safety coefficients of the materials.

3 Seismic performance assessment analysis in current conditions

The performance assessment analysis was carried out for the four reference seismic levels fixed in the Italian Standards [7], that is, Frequent Design Earthquake (FDE, with 81% probability of being exceeded over the reference time period V_R); Serviceability Design Earthquake (SDE, with 50%/ V_R probability); Basic Design Earthquake (BDE, with 10%/ V_R probability); and Maximum Considered Earthquake (MCE, with 5%/ V_R probability). The V_R period is fixed at 50 years, coinciding with the nominal structural life of the structure. By referring to topographic category T1 (flat surface), and C-type soil (deep deposits of dense or medium-dense sand, gravel or stiff clay from several ten to several hundred meters thick), the resulting peak ground accelerations for the four seismic levels referred to the city of Leghorn are as follows: 0.062 g (FDE), 0.08 g (SDE), 0.209 g (BDE), and 0.254 g (MCE), for the horizontal motion components; and 0.011 g (FDE), 0.017 g (SDE), 0.071 g (BDE), and 0.1 g (MCE), for the vertical component. Relevant pseudo-acceleration elastic response spectra at linear viscous damping ratio $\xi=5\%$ are plotted in Fig. 7.

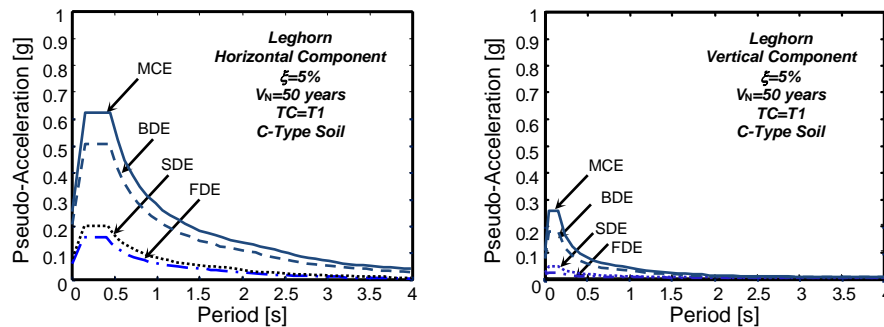


Fig. 7. Normative pseudo-acceleration elastic response spectra for the horizontal and vertical earthquake components – Leghorn.

The time-history analyses were developed by assuming artificial ground motions as inputs, generated in families of seven by SIMQKE-II software [8] from the spectra above, both for the horizontal components (two families) and the vertical one (one family). In each time-history analysis the accelerograms were applied in groups of three simultaneous components, i.e. two horizontal components, with the first one selected from the first generated family of seven motions, and the second one selected from the second family, plus the vertical component.

The finite element model of the structure was generated by SAP2000NL program [9]. A perspective view of the model, reproducing the structural system in elevation, is displayed in Fig. 8.

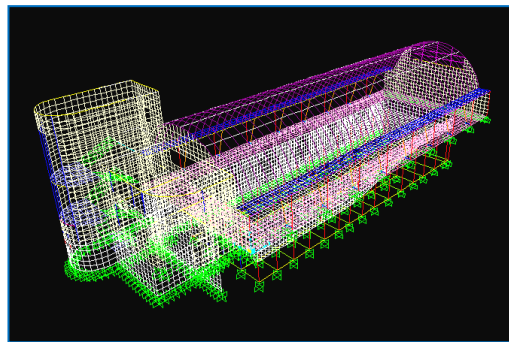


Fig. 8. View of the finite element model of the structure in elevation.

The frame structure bearing the pool tank and the perimeter R/C walls were modelled separately, so as to restrain the dimensions of the mesh within reasonable computational limits. Frame-type elements were adopted to model beams and columns, and shell-type elements for the masonry walls of the stairwell and entrance wings, and the end walls of the pool hall.

A modal analysis of the structure was preliminarily carried out, and showed that all main vibration modes are mixed translational, along the longitudinal and transversal

directions in plan, and rotational, around the vertical axis. The first mode is mainly translational in longitudinal direction, with vibration period of 0.2 s and effective modal mass (EMM) equal to 35.4% of the total seismic mass; the second mode is mainly translational in transversal direction, with period of 0.19 s and EMM of 45.9%; the third mode is mainly rotational, with period of 0.11 s and EMM of 23.1%. 35 modes are needed to obtain summed EMMs greater than 90% along the two directions in plan and around the vertical axis. These data confirm that, as a consequence of the eccentric position of the stairwell and entrance wings in plan, the rotational component remarkably affects the main vibration modes of the structural system.

The seismic assessment investigation was developed by referring to the performance levels established by the Italian Technical Standards, that is, Operational (OP), Immediate Occupancy (IO), Life Safety (LS), and Collapse Prevention (CP), and related evaluation criteria and limitations. The maximum interstorey drift ratio $ID_{r,max}$ (i.e. the ratio of maximum interstorey drift to interstorey height) is assumed as the basic response parameter for the OP and IO levels. The reference drift limits are fixed at 0.33% — OP and 0.5% — IO for the R/C portions of the structural system, and 0.2% — OP and 0.3% — IO for the brick masonry portions, in order to avoid (OP) or keep to a minimum (IO) the seismic damage. The performance evaluation criteria for the LS and CP levels are based on the stress state checks of structural members.

The results of the time-history analyses, elaborated in mean terms over the response to the seven groups of input accelerograms, show $ID_{r,max}$ values below the OP-related and IO-related limitations for the R/C pool hall structure and the masonry wings, at FDE and SDE levels, respectively. The identified FDE–IO, SDE–OP correlations assess a good performance of the building in terms of displacements, as a consequence of the high translational stiffness of the structural system.

The analyses carried out at the BDE level show that stress checks are not met by 25% of columns in compression-bending; 30% of columns in shear; 40% of beams in bending; and 35% of beams in shear. Furthermore, the normal stress exceeds the tensile strength f_{tm} in about 15% of the shell mesh of the masonry walls. Although based on an elastic time-history analysis, these data reveal a high seismic demand on a considerable number of R/C members, and a potentially cracked response of several zones of the masonry wings. This identifies severely damaged response conditions of the building, even though not critical in terms of global structural stability, and thus they correspond to the attainment of the LS performance level at the BDE.

The results of the analyses at the MCE are summarized in the graphs of Figs. 9 through 11. Columns not checked in shear and compression–bending are highlighted in Fig. 9 with blue and pink circles, respectively.

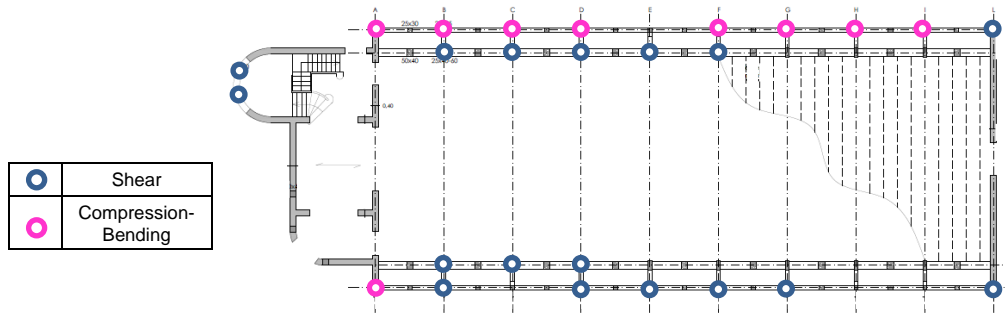


Fig. 9. Summary of columns in unsafe conditions at the MCE.

The histogram in Fig. 10 recapitulates the percent shares of R/C members in unsafe conditions, subdivided in groups. In particular, the numbers tagged on the bars are referred to: 1. roof, façade and stairwell columns in compression–bending; 2. the same columns in shear; 3. façade and roof bearing beams in bending; 4. the same beams in shear; 5. roof V-shaped beams; 6. under-pool columns; 7. under-pool beams.

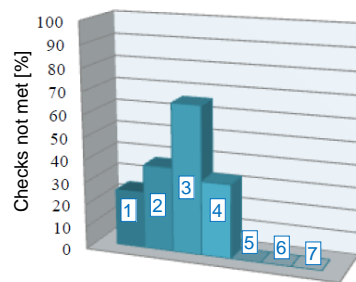


Fig. 10. Histogram of groups of R/C members in unsafe conditions at the MCE.

Consistently with the visual representation in Fig. 9, sets 1 and 2 in Fig. 10 are equal to 25% and 35%, respectively, with 50% of columns not checked either in compression–bending or in shear (10% do not meet either verifications). Sets 3 and 4 are equal to 70% and 30%, with 100% of unsafe beams in total (10% do not meet either verifications in this case too). All R/C members belonging to groups 5, 6 and 7 pass relevant stress checks.

The portions of the entrance wing–stair wing–pool lateral wall meshes where the vertical normal stress is lower than f_{tm} are plotted in light yellow in Fig. 11. The extension of the remaining zones, implicitly subjected to crack openings, is equal to about 30% (i.e. increased by a factor 2 as compared to the BDE-induced response). The stress peaks, situated around the windows of the pool lateral wall and at the bottom of the internal and external walls of the entrance wing, are up to three times greater than f_{tm} .

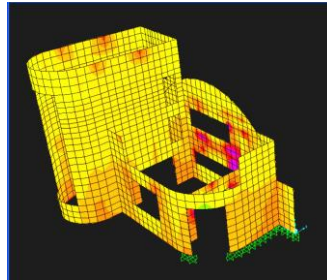


Fig. 11. Vertical normal stress contours of the entrance wing–stair wing–pool lateral wall mesh obtained from the most demanding MCE-scaled group of input accelerograms.

By jointly evaluating the output data of the analyses at the MCE, a relatively poor performance comes out, only just meeting the minimal requirements of the Collapse Prevention level.

The results of the evaluation study at the two highest earthquake levels, synthesized by the BDE–LS and MCE–CP correlations, prompted to examine proper retrofit hypotheses aimed at improving the assessed performance, while at the same time being respectful of the architectural value of the building. Consistently with this requirement, a seismic isolation solution was designed, so as to obtain null impact on the structural members in elevation. As observed in the Introduction, this solution was also suggested by the easy installation determined by the presence of the frame structure bearing the pool tank and the perimeter interspace of the basement volume.

4 Seismic isolation retrofit proposal

The proposed system includes double curved sliding surface (DCSS) bearings as isolation devices, a schematic section and two views of which are shown in Fig. 12.

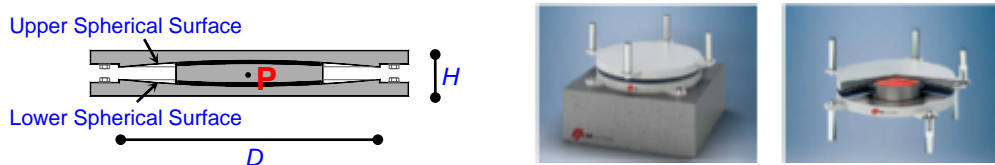


Fig. 12. DCSS isolator type adopted for the seismic isolation retrofit hypothesis.

DCSS isolators have been proposed and implemented with the aim of remarkably reducing dimensions as compared to single curved sliders designed for the same objectives [10], which is a very useful quality especially for installation in existing R/C structures [5,11].

The positions of the isolators incorporated in the case study building are highlighted with red circles in the plan of Fig. 13. The sliders are placed on top of

each column of the under-pool structure (60 elements), at the bottom of each pair of façade columns-roof columns (16 elements), and below the stairwell/entrance wing walls and the lateral walls of the pool hall (19 elements). This results in a multi-level geometrical isolation plane, marked by red lines in the longitudinal cross section drawn in Fig. 13. The plane is constituted by the continuous R/C slabs of the pool tank and hall, plus the ground story slab of the masonry wings. The mutual 300 mm thickness of these slabs warrants an effective rigid diaphragm function of the plane, as required for the best performance of any isolation system.

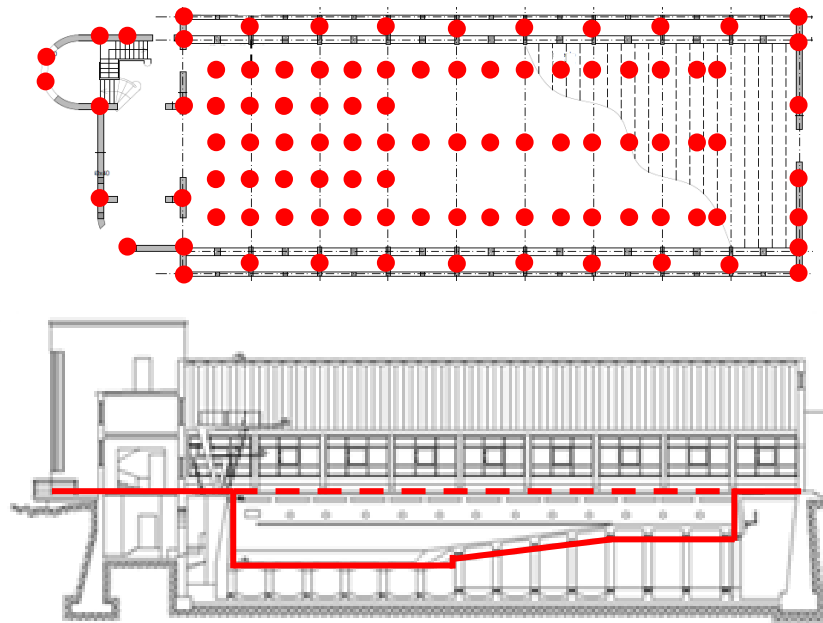


Fig. 13. Plan with the positions of the DCSS isolators (red circles) and longitudinal cross section highlighting the geometrical layout of the multilevel isolation plane.

As a consequence of the relatively small tributary areas to gravitational loads of the under-pool columns, as well as of the lightweight barrel vault of the hall, the required axial force-resisting surface of the isolators is provided by the smallest type of DCSS devices in standard production by the selected manufacturer [12]. The mechanical and geometrical properties of this model are as follows: effective pendulum length $L_{DFP}=2535$ mm; maximum displacement capacity $d_{max}=\pm 200$ mm; friction coefficient of the sliding surfaces $\mu=0.025$; equivalent vibration period of the isolator at the maximum displacement $T_e(d_{max})=2.78$ s; equivalent viscous damping ratio at the maximum displacement $\xi_e(d_{max})=15.2\%$; plan diameter of the concave surfaces $D=400$ mm; H =height=84 mm; and maximum dimension in plan including the connection flanges $D_c=450$ mm.

The D_c value allows mounting the isolators on top of the under-pool columns and at the bottom of the façade-roof column pairs (i.e. on top of the underlying basement wall) without enlarging relevant bearing members. At the same time, a

500 mm-wide R/C edge beam must be built at the base of the masonry walls before incorporating the isolators. By way of example, the installation details of a device below the façade-roof columns are shown in the drawing of Fig. 14, highlighting that demolitions are limited to a 130 mm-thick top portion of the basement wall.

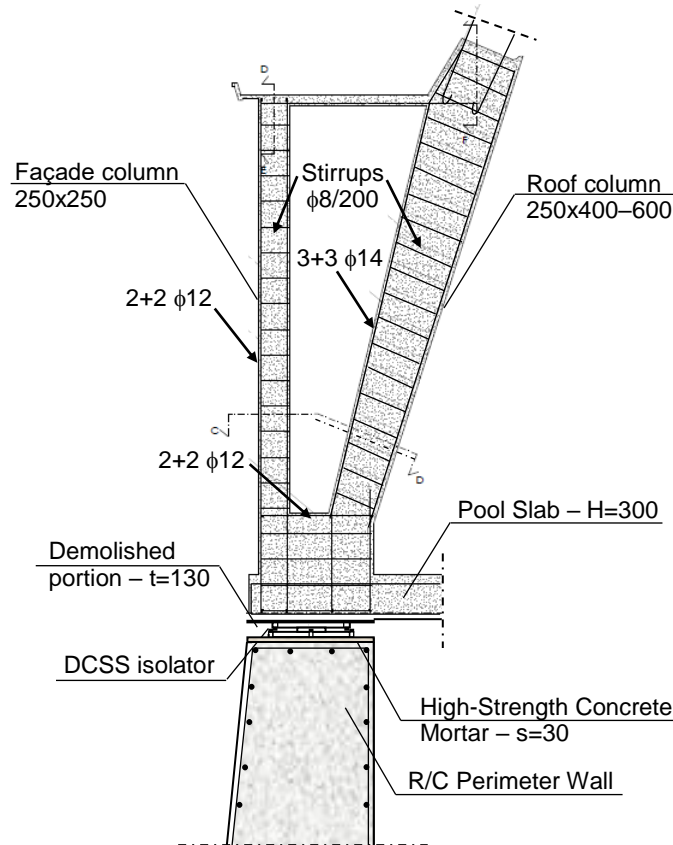


Fig. 14. Installation details of an isolator at the bottom of a façade-roof column pair.

For the development of the time-history analyses in seismically isolated configuration, the finite element model of the DCSS devices was generated by the special “Friction Isolator” link element available in the library of SAP2000NL software. This is a biaxial friction-pendulum element with coupled friction properties for the deformations along the two reference local axes in plan, and “gap”-type behaviour in vertical direction.

The first two vibration modes in isolated conditions are essentially translational along the longitudinal direction (first mode) and the transversal direction (second mode), with periods of 2.82 s (first) and 2.81 s (second). The two values are very similar to the equivalent period of the isolators, $T_e(d_{max})$, as a consequence of the negligible contribution of the superstructure deformability to these modes. The modal masses are nearly equal to 100% of the total seismic mass in both directions.

The third mode is purely rotational, with period of 2.6 s, and EMM equal to about 100% of the seismic mass too.

The performance evaluation enquiry carried out in original conditions was duplicated in the base isolation retrofit hypothesis. The good response at the two lowest earthquake levels assessed in current state is improved further thanks to the protective intervention, reaching the OP limit state at SDE too, in addition to the FDE.

Concerning the BDE and MCE levels, all R/C members result to be within their safe domain, and the normal stress peaks in the masonry walls below f_{tm} , in isolated conditions. The latter result is visualized in the mesh view of Fig. 15, where the elements with stress values lower than f_{tm} are plotted in purple.

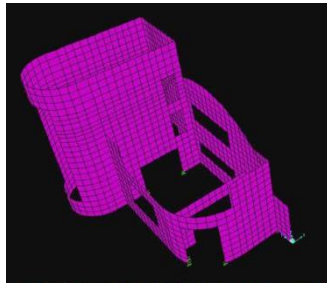


Fig. 15. Vertical normal stress contours of the entrance wing–stair wing–pool lateral wall mesh obtained from the most demanding MCE-scaled group of input accelerograms in isolated conditions.

The peak displacements of the DCSS isolators were checked at the MCE level. The response cycles obtained from the most demanding group of input accelerograms for three devices, placed on top of the under-pool columns, at the bottom of the façade-roof column pairs and at the bottom of the stairwell wing, respectively, are plotted in Fig. 16.

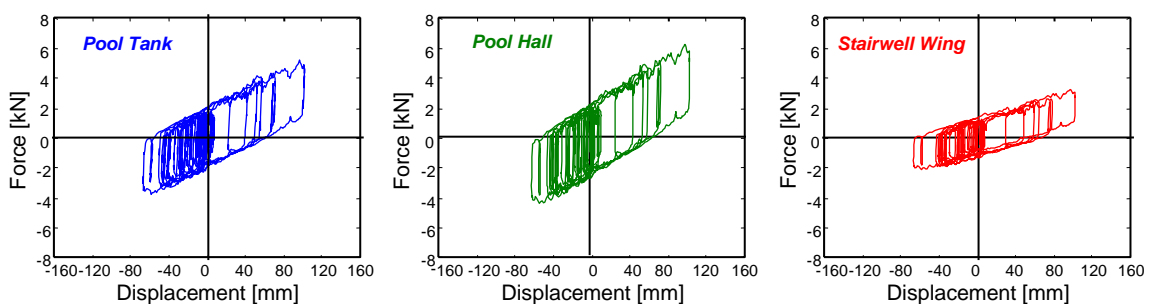


Fig. 16. Response cycles of three isolators obtained from the most demanding MCE-scaled group of input accelerograms.

A mutual maximum displacement of about 100 mm is recorded, i.e. half the isolator capacity $d_{max} = \pm 200$ mm. The responses of the three devices are practically coincident and in-phase in terms of displacements, underlining that the retrofitted

structure is substantially unaffected by plan torsion effects. The differences in terms of forces and stiffness are related to the different axial forces acting on the isolators.

The displacement capacity/demand ratio equal to about 2:1 guarantees adequate safety margins with respect to the physical effects not modelled in the analysis, among which a decrease in nominal friction coefficient due to the simultaneous three-directional seismic excitation, and the start of sliding of the two surfaces at different times, caused by possible unequal sticking.

5 Conclusions

The study carried out on the swimming pool building of the Naval Academy in Leghorn assesses a relatively satisfactory performance of the structure at the FDE and SDE, identified by FDE–IO and SDE–OP correlations, as a consequence of its high elastic translational stiffness.

On the other hand, at the BDE either compression or shear stress checks are not met by 30% of columns and 40% of beams, and the normal stress exceeds the tensile strength in about 15% of the masonry wall meshes, outlining the attainment of the LS performance level.

The increased number of unsafe R/C members and the wider extension of potentially cracked zones of masonry walls surveyed at the MCE, in comparison to the BDE, allow meeting only the minimal requirements of the CP limit state.

Based on these data, targeting and reaching a substantial seismic performance improvement would imply notably intrusive interventions, not respectful of the architectural value of the building, should traditional rehabilitation techniques be adopted. Therefore, a seismic isolation retrofit hypothesis was proposed, so as to generate a null impact on the structural members in elevation.

This solution allows reaching safe response in all R/C members and tensile stress distributions below relevant strength in all masonry walls, thus identifying BDE–IO and MCE–IO correlations.

The technical and economic feasibility of the intervention are favoured by the possibility of easily installing the isolation system, owed to the presence of the frame structure bearing the pool tank and the perimeter interspace of the basement volume.

Hopefully, this will help adopt the same strategy for other R/C vaulted structures built in seismic areas during the “golden-age” decades.

Acknowledgements. The study reported in this paper was financed by the Italian Department of Civil Protection within the ReLUIIS-DPC Project 2016, Research Line 6: Isolation and Dissipation. The authors gratefully acknowledge this financial support.

References

- [1] S. Sorace and G. Terenzi, Structural assessment of a modern heritage

- building, *Engineering Structures*, **49** (2013), 743-755.
<http://dx.doi.org/10.1016/j.engstruct.2012.12.012>
- [2] A. Custance-Baker and S. Macdonald, *Conserving Concrete Heritage*, The Getty Conservation Institute, Los Angeles, CA, 2014.
- [3] S. Sorace and G. Terenzi, Dissipative bracing-based seismic retrofit of R/C school buildings, *The Open Construction and Building Technology Journal*, **6** (2012), 334-345. <http://dx.doi.org/10.2174/1874836801206010334>
- [4] F. Mazza, Modelling and nonlinear static analysis of reinforced concrete framed buildings irregular in plan, *Engineering Structures*, **80** (2014), 98-108. <http://dx.doi.org/10.1016/j.engstruct.2014.08.026>
- [5] S. Sorace, G. Terenzi and C. Mori, Passive energy dissipation-based retrofit strategies for R/C frame water towers, *Engineering Structures*, **106** (2016), 385-398. <http://dx.doi.org/10.1016/j.engstruct.2015.10.038>
- [6] Italian Council of Public Works, *Commentary on the Technical Standards on constructions* [in Italian], Rome, Italy, 2009.
- [7] Italian Council of Public Works, *Technical Standards on Constructions* [in Italian], Rome, Italy, 2008.
- [8] E.H. Vanmarcke, G.A. Fenton and E. Heredia-Zavoni, *SIMQKE-II-conditioned earthquake ground motion simulator: User's manual*, version 2.1, Princeton University, Princeton, New Jersey, 1999.
- [9] CSI, *SAP2000NL, Structural analysis programs- Theoretical and users manual*, Release no.17.06, Berkeley, California, 2016.
- [10] D.M. Fenz and M.C. Constantinou, Behaviour of the double concave friction pendulum bearing, *Earthquake Engineering and Structural Dynamics*, **35** (2006), 1403-1424. <http://dx.doi.org/10.1002/eqe.589>
- [11] S. Sorace and G. Terenzi, A viable base isolation strategy for the advanced seismic retrofit of an R/C building, *Contemporary Engineering Sciences*, **7** (2014), 817-834. <http://dx.doi.org/10.12988/ces.2014.4549>
- [12] FIP, *Anti-seismic devices product division* 2016.
<http://www.fip-group.it>